

# Comparative study on the time-domain analysis of non-linear ship motions and loads

I. Watanabe<sup>a,\*</sup>, C. Guedes Soares<sup>b</sup>

<sup>a</sup>*Ship Research Institute, Ministry of Transport, 6-38-1 Shinkawa, Mitaka, Tokyo, Japan*

<sup>b</sup>*Unit for Marine Technology and Engineering, Technical University of Lisbon, Instituto Superior Técnico, Av. Rovisco Pais, 1049-001 Lisboa, Portugal*

Received 1 February 1999; received in revised form 15 March 1999; accepted 6 April 1999

---

## Abstract

A benchmark study has been performed by comparing the predictions of different non-linear time-domain codes applied to study the vertical wave-induced bending moment in a container-ship in waves of different steepness. Most methods are based on strip theory formulations applied both to rigid-body and to flexible hull formulations, but one adopts a 3-D formulation.

It has been shown that the results are consistent with the linear estimates in the lower wave height region. However, the agreement among the computed values becomes poor in the higher wave region when the elastic behaviour of the hull plays a significant role. © 1999 Elsevier Science Ltd. All rights reserved.

*Keywords:* Hydroelasticity; Non-linear wave load; Time-domain simulation

---

## 1. Introduction

The tendency of substituting rule based values for the design of ship structures by values directly calculated for each individual ship, will allow the specific features of ships to be considered in design, but has the drawback that for the same ship the use of different computer codes may yield different values of the wave-induced loads [1].

Although the linear strip theory has been established many years ago as an adequate design tool for the assessment of wave-induced loads on ships, it has also been known that it has some limitations, one of which is its linear nature. Despite the widespread use of the theory it has been shown that the different codes based on it

---

\* Corresponding author.

yield different predictions, which can be considered a modelling uncertainty from a design point of view [2].

As far back as in 1966 Smith [3] has reported on the results of full-scale measurements of wave induced loads on destroyers, which has clearly shown that the sagging moments experienced are much larger than the hogging ones. Since then, several efforts have been made to develop theories that are able to represent this non-linear feature of the wave loading process. In general one can group these efforts in approaches that attempt to model in a detailed and accurate form all non-linearities and another group that includes the methods which attempt to account only for the most significant contributions in a physically based approach similar to strip theory.

The first type of approaches have a good future potential but in the short term they require very heavy computations and thus are not adequate for application in design oriented studies. For design purposes it is more attractive to use the approaches that require more limited computational effort, which in general is only achievable with different modifications of strip theory.

Many of the approaches to non-linear load prediction are based on time-domain simulation of ship responses in extreme wave conditions. Time simulation techniques are expected to become increasingly more popular as the capability of computers are developed further.

The methods to simulate in the time-domain responses of the ships in waves can be divided in two main groups. The first one includes the more advanced numerical procedures, in which the hydrodynamic problem is solved directly in the time-domain. In general these methods have three levels of complexity, with increasing computational effort to obtain the solution.

In the first level the underwater geometry does not change in time and all hydrodynamic forces are linear as well as the ship responses in waves. In this case the boundary value problem is solved only once and the hydrodynamic quantities are then reused at each time step.

In the second level, the hydrodynamic problem remains linear but the hydrostatic restoring and Froude–Krilov forces are evaluated under the incident wave elevation.

In the third level the underwater body geometry changes with time, thus the hydrodynamic terms are computed using the exact-body boundary condition applied at the instantaneous wetted surface. The free surface condition is retained, linearized around the mean wave surface or around the incident wave surface. This approach results in very intensive computational effort.

These more advanced numerical procedures can be further divided in 3D Green function methods [4,5], 3D Rankine source methods (Kring and Sclavounos [12]) and the desingularized method [6].

Using transient Green function methods only the hull boundary needs to be discretized. The singularities, which are located on the discretized boundary, satisfy the free surface boundary condition. An alternative to the use of Green functions is the use of Rankine sources. These singularities, being much simpler to calculate, do not satisfy the free surface boundary condition, thus the discretized domain must be extended to the free surface.

The desingularized method is under development to tackle the fully non-linear three-dimensional free surface problem. In this method fundamental singularities are distributed over an “integration surface” and enforced at collocation points of a “control surface”. In other methods the integration and control surfaces are the same, which results in singular kernels. By this method the kernels become desingularized, thus no special treatment is required for evaluating the integrals. Results of radiation and exciting forces calculated by this method were presented by Beck et al. [7] and Scorpio et al. [6].

A numerically less intensive time-domain solution was presented by Zhao and Aarsnes [8] which is based on a  $2\frac{1}{2}$ D approach. Basically a two-dimensional Laplace equation is assumed, but the free surface conditions are three-dimensional. An assumption is used that there are no upstream waves generated by the body far away from the ship ( $\tau = \omega_e U/g > 0.25$ ). The exact-body boundary condition is used together with a free surface condition linearized around the incident wave elevation.

In the second main group of time-domain simulation procedures, the hydrodynamic problem is linear and basically solved in the frequency domain. The restoring hydrostatic and Froude–Krilov terms are evaluated over the instantaneous wetted surface. Effects like slamming, deck wetness, directional control and others can be introduced in the equations of motion. The linear and non-linear terms are joined together in the equations of motion, which are solved in the time-domain to obtain the non-linear responses. Also the vibratory response of the hull to slamming impacts can be incorporated in the simulation or in a post-processing basis.

Differences between the methods are found on the way the frequency domain results are used to represent the hydrodynamic forces in the time-domain, on the use or not of the relative motion concept, and on the way that the non-linear effects mentioned above are introduced. Most of these procedures are based on strip theory approaches, which are relatively simple to implement and the solutions involved limited computational efforts.

Examples of such methods in which the hydrodynamic forces are represented by memory functions obtained by Fourier transforms of frequency domain results are the ones proposed by Fonseca and Guedes Soares [9,10] and by Xia et al. [11]. Watanabe et al. [12] and Tao and Incecik [13,14] proposed methods in which the hydrodynamic forces are dependent of the instantaneous sectional immersion and represented by frequency dependent coefficients.

The procedures under study in the present paper all belong to this last group of more simplified methods.

This paper reports the results of a comparative study on the performance of different codes for evaluation of non-linear loads in ships. The adequacy of each theory is normally evaluated by comparing its predictions with experimental results, which are not abundant when concerned with non-linear loads. Thus, the comparisons provided here will not allow conclusions to be extracted about the accuracy of the methods, but they will provide an indication about the model uncertainty involved in their application.

## 2. Description of the methods

This paper presents a comparison of non-linear time-domain simulation programs from different organizations. Six organizations participated in the study, performing the calculations with their own codes. They are University of Newcastle [13], the Technical University of Lisbon (Instituto Superior Técnico), Fonseca and Guedes Soares, [9,10] (IST1) and Ramos and Guedes Soares, [15] (IST2), Det Norske Veritas, [16], China Ship Scientific Research Centre [11], Kanazawa Institute of Technology [17] and the Ship Research Institute of Japan [12].

The method of Kring et al. [16] is a three-dimensional time-domain program for arbitrary-shaped ships (including multi-hulls) or other main structures in waves. The ship may have an arbitrary forward speed, the waves can come from any direction and the responses can be computed in all six degrees of freedom. The program is based on a three-dimensional Rankine panel method. Radiation conditions are treated by including a zone where the free surface condition is modified such as the waves are absorbed, i.e. a numerical beach. Important non-linear effects included are: hydrostatics, Froude–Krylov force, inertia and gravity effects, water on deck and roll damping.

The other programs are based on modifications of the strip theory but different choices have been made about the features to include in the formulation, as summarised in the Table 1. A brief description is given to clarify some key points of the formulations that are the basis of the programs treated here.

Table 1  
Main features of the methods considered in the study

Methods	Newcastle	IST1	IST2	DNV	CSSRC	KIT	SRI
Elastic hull	No	No	Yes	No	Yes	Yes	Yes
Non-linear motions	Yes	Yes	No	Yes	Yes	Yes	Yes
Non-linear hydrostatic	Yes	Yes	No	Yes	Yes	Yes	Yes
Non-linear Froude–Krilov	No	Yes	No	Yes	Yes	No	Yes
Non-linear added mass and damping	Yes	No	No	Yes	No	Yes	Yes
Relative motion concept	No	No	Yes	No	No	No	Yes
Smith correction	Yes	No	No	Yes	Yes	Yes	Yes
Linear diffraction exciting forces	No	Yes	No	Yes	No	No	No
Non-linear diffraction exciting forces	No	No	No	Yes	No	No	No
Free surface memory effects	No	Yes	No	No	Yes	No	No
Slamming loads by bottom slamming	No	No	Yes	No	No	Yes	Yes
Slamming loads by momentum slamming	Yes	No	Yes	No	Yes	Yes	Yes
Water on deck	No	Yes	No	Yes	No	No	Yes

Elastic hull means that the transient vibratory response of the hull to the slamming impact loads is calculated. Non-linear motions mean that at least one of the force components in the equations of motion is non-linear.

The hydrostatic and Froude–Krilov forces are non-linear if the corresponding pressures are evaluated over the “exact” immersed hull. In the present study, non-linear added mass and damping means that the assumed frequency-dependent sectional coefficients are dependent of the instantaneous immersion. The relative motion concept and Smith effect will be described in the next section of the text.

When diffraction-exciting forces are considered, it means that the wave exciting problem is solved by formulating and solving the appropriate boundary value problem and considering the body and free surface boundary conditions. If these forces are dependent of the instantaneous immersion then they are non-linear.

Most of the programs assume the hydrodynamic coefficients to be equal to those at the characteristic frequency such as mean frequency or to those at infinite frequency. However, some programs make use of memory functions in order to take “memory effects of the free surface” into consideration. If the radiation forces are represented by convolution of memory functions instead of frequency dependent coefficients, then the free surface memory effects are considered.

The slamming loads may be calculated using the bottom slamming approach or momentum slamming approach. Finally the effects of water on deck may also be considered for the calculation of motions and structural loads.

### 2.1. Relative motion concept

For the calculation of the external hydrodynamic forces some programs use the relative motion concept and some do not. The relative motion concept considers that the hydrodynamic forces are dependent solely on the relative motion between the hull and water wave. Let  $r$  be the relative motion defined by

$$r = \zeta - \zeta_w,$$

where  $\zeta$  is the vertical displacement of the ship section and  $\zeta_w$  is the wave elevation. The typical formulation for the external force is

$$F_s(x, r) = \rho g(A(x, r) - A_0(x)),$$

$$F_d(x, r) = -\frac{d}{dt} \left( m(x, r) \frac{dr}{dt} \right) - N(x, r) \frac{dr}{dt}.$$

Here  $m(x, r)$  and  $N(x, r)$  are the added mass coefficient and the damping coefficient of the section at  $x$  with relative water displacement  $r$ .

The left-hand side may be broken into two parts as

$$F_d(x, r) = -m(x, r) \frac{d^2r}{dt^2} - N(x, r) \frac{dr}{dt} - \frac{\partial m}{\partial t} \frac{dr}{dt}.$$

The first two terms correspond to ordinary linear terms while the third term, corresponds to the impact term, the so-called momentum slamming term.

The impact force is expressed as the rate of change of the added mass with the immersion of the body.

Some of the programs do not use the relative motion concept. In this case the formulation for the hydrodynamic forces results from the linearization of the potential flow problem. The general hydrodynamic problem is simplified to three independent problems; the radiation problem, the diffraction problem and the hydrostatic problem.

In the case of the radiation and hydrostatic problems, the ship is assumed to be advancing with forward speed and oscillating on the free surface. The incident waves are not considered. The hydrodynamic forces are dependent of the absolute motions, velocities and accelerations.

In the case of the diffraction problem, the ship is assumed to be advancing on the free surface and restrained at its mean position. The hydrodynamic exciting forces comprise the Froude–Krilov part and the diffraction part.

In order to account for the variation of the immersed volume of the hull with the large amplitude relative vertical motions, the hydrostatic and Froude–Krilov forces are calculated over the instantaneous wetted surface of the below the incident wave. To keep the simplicity of the solution the radiation and diffraction forces are kept linear.

## 2.2. Elastic hull

Some programs take care of elastic mode of motion together with rigid body modes but others account for rigid body modes only. They can be regarded as a special case of the elastic body formulation.

The hull structure is assumed to be a Bernoulli beam with varying elastic rigidity. The balance of forces for a section at a longitudinal location ( $x$ ) at each time sequence can be described as follows:

$$m \frac{\partial^2 \zeta}{\partial t^2} + EI(x) \left( \frac{\partial^4 \zeta}{\partial x^4} + \varepsilon \frac{\partial^5 \zeta}{\partial t \partial x^4} \right) = F_s(x, \zeta) + F_d(x, \zeta),$$

where  $m$  is the mass per unit length,  $EI$  the bending rigidity of the beam and  $\varepsilon$  is related to the visco-elastic properties of the beam.

Here  $\zeta$ , the vertical displacement of the hull section is comprised of rigid mode motion and elastic mode motion. The second term of the left-hand side will be omitted if the elasticity is neglected.

The right-hand side terms denote the external force components.  $F_s(x)$  is the force component due to hydrostatic origin and the gravitation,  $F_d(x)$  is the hydrodynamic component which include components due to ship motion and wave action. Non-linear hydrodynamic terms due to slamming or other non-linear phenomena appear here if included in the model.

In most of the methods the solution of the non-linear equations of motion is advanced in the time-domain and the induced bending moment calculated simultaneously. However, there is another way of formulation, where the linear equations of rigid-body motion are solved first and then the bending moments when slamming

loads occur are calculated. The low-frequency wave-induced moment is calculated at this step. On the second step the impact forces and the hull structure response are calculated [15], modelling the hull as a flexible structure.

### 3. Description of the reference conditions

#### 3.1. Ship characteristics

The S-175 container ship was selected as the hull to be studied. The model was chosen because the hull form data and experimental data can be easily obtainable, since they have been used, among others, for an ITTC comparative study. The main particulars of the reference ship are: ship length ( $L$ ) = 175 m; breadth ( $B$ ) = 25.4 m; draft ( $d$ ) = 9.5 m and displacement ( $W$ ) = 24742 T.

The body plan of the model is given in Fig. 1.

When the vertical bending elasticity of the hull girder is taken into account, the logarithmic damping coefficient of elastic vibration is assumed 0.051 for all modes of vibration.

#### 3.2. Weight distribution

Trapezoidal form with constant value in the middle part from SS2.5 through SS7.5 and linear attenuation toward FP and AP is assumed. Schematic view is shown in Fig. 2, where  $w$  denotes the averaged weight distribution  $W/L$ .

#### 3.3. Running conditions

Ship speed for the study was set to  $F_n = 0.25$ . For wave conditions, it was agreed to select only regular wave and head sea cases.

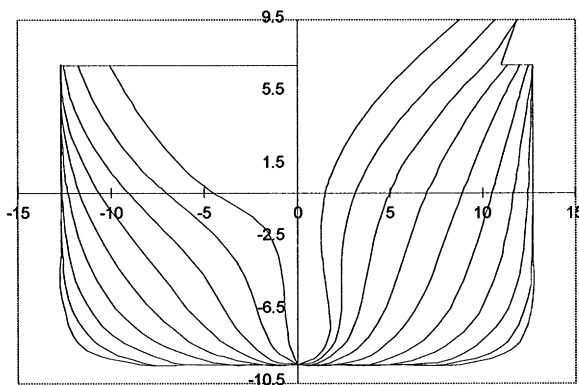


Fig. 1. Body plan of the S175 containership.

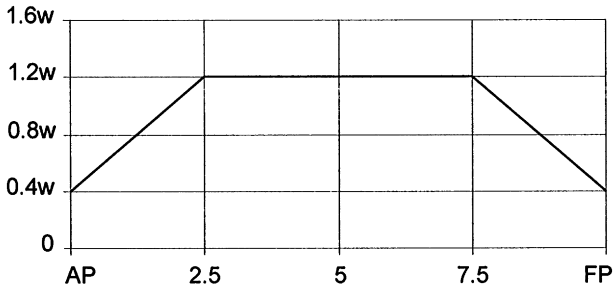


Fig. 2. The weight distribution.

Table 2  
Wave conditions for the calculations

Wave Length ( $WL/L$ )	0.5	1.0	2.0
Wave Height Ratio ( $WH/WL$ )	1/30	1/20	1/10

The wave conditions are taken from combinations of following values of wave length and wave slopes as shown in Table 2.

### 3.4. Items calculated

All participants were requested to submit the time history of pitching motion, relative wave motion at FP and AP, vertical acceleration at FP, midship and AP and vertical bending moments at SS7.5, SS5 and SS2, together with longitudinal distributions of maximum hogging and sagging moment for one cycle of encounter wave frequency.

## 4. Results and discussion

In the following presentation the responses are given in a dimensional form. Pitching in *degrees*, vertical acceleration in  $m/s^2$ , relative water motion in m and vertical bending moment in KN m, being the hogging positive.

### 4.1. Amplitude

Table 3 shows the computed results summarized in the form of double amplitude. Here the double amplitude is defined as the difference between maximum and minimum peaks since the calculated response is not monochromatic due to non-linear behaviour even if the input signal, encounter wave is sinusoidal.



Table 3  
Results of calculations

WL/SL	WH/WL	ITEM	A	B	C	D	E	F	B*	Linear
			Elastic	Elastic	Elastic	Elastic	Elastic	Rigid	Rigid	
0.5	1/30	PITCH	0.32	0.24	0.35	0.60	0.32	0.11	0.24	0.30
		RwFP	2.81	2.88	2.93	3.23	2.73	1.80	2.88	2.83
		RwAP	2.81	2.78	2.67	3.22	2.75	1.66	2.79	2.39
		VaFP	1.28	1.22	1.30	1.44	1.49	0.50	0.96	1.17
		VaAP	1.43	1.18	1.36	1.28	1.23	0.37	0.96	1.19
		VBM7.5	1535	5491	3329	4210	5036		4753	6139
	1/20	VBM5	4633	5593	6506	8518	7265		2405	2900
		VBM2	3424	5332	6979	4907	5141		4640	3846
		PITCH	0.47	0.34	0.51	0.57	0.50	0.19		0.48
		RwFP	4.24	4.33	4.38	4.51	4.11	2.56		4.24
		RwAP	4.19	4.13	3.91	4.55	4.13	2.51		3.57
		VaFP	1.92	1.47	1.91	1.82	2.27	0.75		1.75
1.0	1/30	VaAP	2.16	1.39	2.02	1.70	1.87	0.56		1.78
		VBM7.5	2892	8185	5139	6773	7555			9209
		VBM5	7205	6211	10493	11833	10897			4349
		VBM2	5154	6738	10010	6964	7712			5768
		PITCH	6.89	7.96	7.41	6.90	8.82	4.50	7.96	10.19
		RwFP	16.85	19.13	18.01	15.08	19.44	4.86	19.13	22.39
	1/20	RwAP	4.85	7.06	5.89	6.23	8.04	2.27	7.03	8.86
		VaFP	13.54	13.50	11.75	11.27	13.29	7.18	12.60	16.20
		VaAP	11.66	12.36	10.91	10.12	13.01	0.97	11.44	14.31
		VBM7.5	67208	52741	45778	46847	23397		47631	37390
		VBM5	100841	113622	112633	131374	90705		95165	87621
		VBM2	61965	27033	26321	29407	38021		19630	15491
2.0	1/30	PITCH	8.57	10.73	9.33	10.24	10.18	6.87		15.30
		RwFP	21.46	26.41	22.98	23.41	22.64	6.84		33.60
		RwAP	5.22	9.06	6.93	7.96	8.46	3.59		13.30
		VaFP	16.29	20.96	14.84	19.78	14.37	10.66		24.35
		VaAP	16.43	16.97	14.99	17.43	15.53	1.49		21.46
		VBM7.5	98388	88313	113668	103723	38062			56085
	1/20	VBM5	151072	172032	241764	266613	140385			131432
		VBM2	98810	42084	65030	53390	58977			23237
		PITCH	13.07	12.23	13.34	13.76	13.78	7.64	12.22	13.71
		RwFP	21.57	17.37	23.27	22.76	20.84	4.60	17.38	20.60
		RwAP	8.12	8.60	7.54	9.22	9.92	1.85	8.59	9.64
		VaFP	10.54	9.81	11.16	10.90	10.19	6.89	9.12	10.00
1/30	VaAP	7.87	8.23	7.44	8.16	9.00	11.75	8.11	7.51	
	VBM7.5	49111	50386	54775	26579	24399		46420	18250	
	VBM5	114170	89894	94260	68093	67276		85066	71540	
	VBM2	40363	24211	32762	12575			22470	27879	
	PITCH	19.01	17.84	16.78	20.50	20.94	12.57		20.61	
	RwFP	34.15	26.49	38.17	33.99	35.89	6.90		30.88	
1/20	RwAP	11.24	11.81	8.60	13.62	14.07	3.74		14.46	
	VaFP	18.26	14.43	18.94	17.17	16.03	11.13		15.00	
	VaAP	13.05	12.74	11.86	14.62	13.85	19.19		11.27	
	VBM7.5	82951	67567	227798	47721	40956			27375	
	VBM5	179782	139790	342454	136347	109648			107310	
	VBM2	66544	40471	163686	28115				41819	

A, B, C, D, E and F in the first row denote each organisation and the last column shows linear estimates by linear strip method. In Table 3 R<sub>w</sub>FP and R<sub>w</sub>AP denotes the relative wave height at the forward and often perpendicular, respectively, V<sub>a</sub>FP and V<sub>a</sub>AP are the vertical acceleration at those locations and VBM are the vertical bending moment at the sections 7.5, 5 and 2. It is seen that agreement among non-linear estimates and linear estimates is fairly good in lower wave height regime but becomes poor as the waves become higher.

Fig. 3 shows the variation of double amplitude of relative water at FP to the wavelength. The amplitude is non-dimensionalized by the wave height in this figure. Results of non-linear computation denoted by symbols are scattered around the linear estimation by the strip method denoted by solid line for all combinations of wave height and wavelength. It is seen that most programs are capable to explain the response variation to the wavelength but give scattered values quantitatively. The results include both elastic rigid body estimation and rigid-body estimation. There seems to be no difference in the quality of the estimation by including elastic effects.

In order to show how the amplitude of relative water at FP varies to the wave height change Fig. 4 was prepared. The dotted line shows the linear predictions for reference. The amplitude is denoted in meters in this figure. It is seen that most of the non-linear estimates are lower than linear estimates. This may be explained by the fact

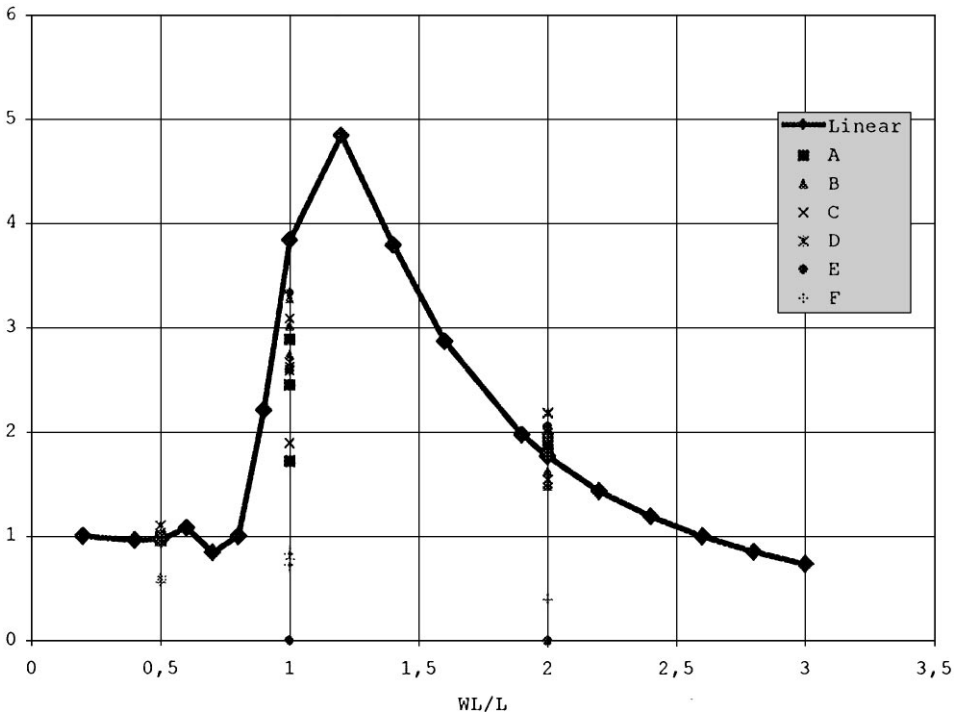


Fig. 3. Comparison of computed amplitude of relative water elevation at FP.

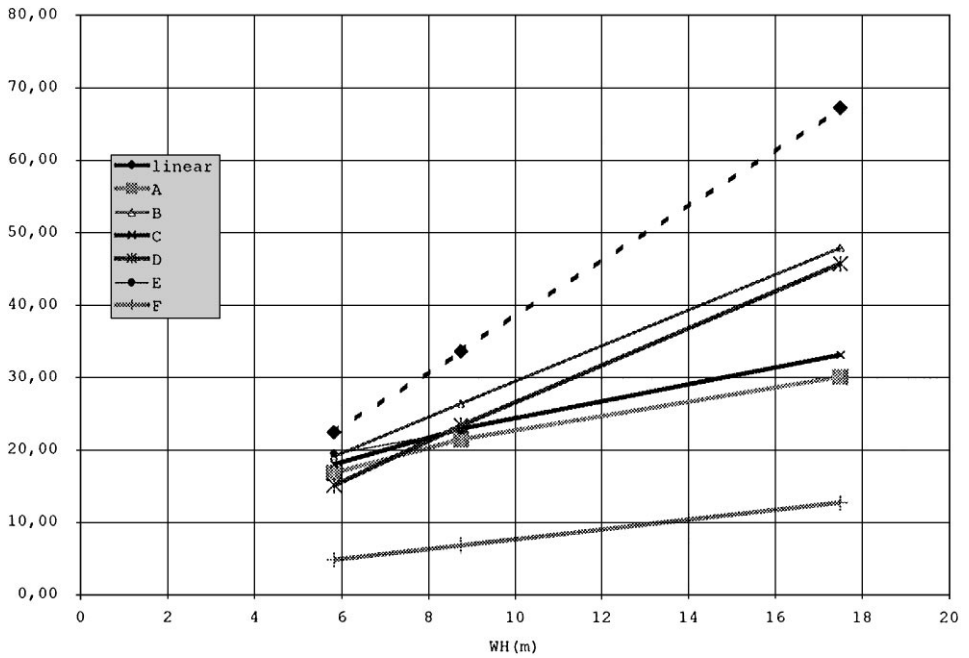


Fig. 4. Variation of relative water elevation at FP wave length ratio = 1.

that when relative motion at the bow is developed to the extent to exceed draft and freeboard there, the bow emergence and deck submergence introduces non-linear force change suppressing vertical motion. Most programs seem capable to take care of this non-linearity but in a slightly different manner judging from the difference in the amplitudes computed.

The non-linear components are more significant in responses such as vertical acceleration and bending moment since they may be easily influenced by elastic behaviour. Fig. 5 shows how the amplitude of the vertical bending moment (VBM) at the midship varies to the wave height change. Dotted line shows linear estimation for reference. It is seen that the non-linear estimates are in line with the linear estimates when the wave height is relatively low but give higher estimates than the linear ones in high wave height region. This is possibly the cause by non-linear responses such as non-linear change of the submerged part, slamming and subsequent whipping motion of the hull.

#### 4.2. Distribution of maximum hogging and sagging moment

Fig. 6 shows the longitudinal distribution of bending moment computed by the programs. Maximum hogging and sagging moments during one encounter wave cycle are plotted. It is seen that the programs give wide scattering of estimates in spite of similar distribution shape. The differences are pronounced because a slight difference

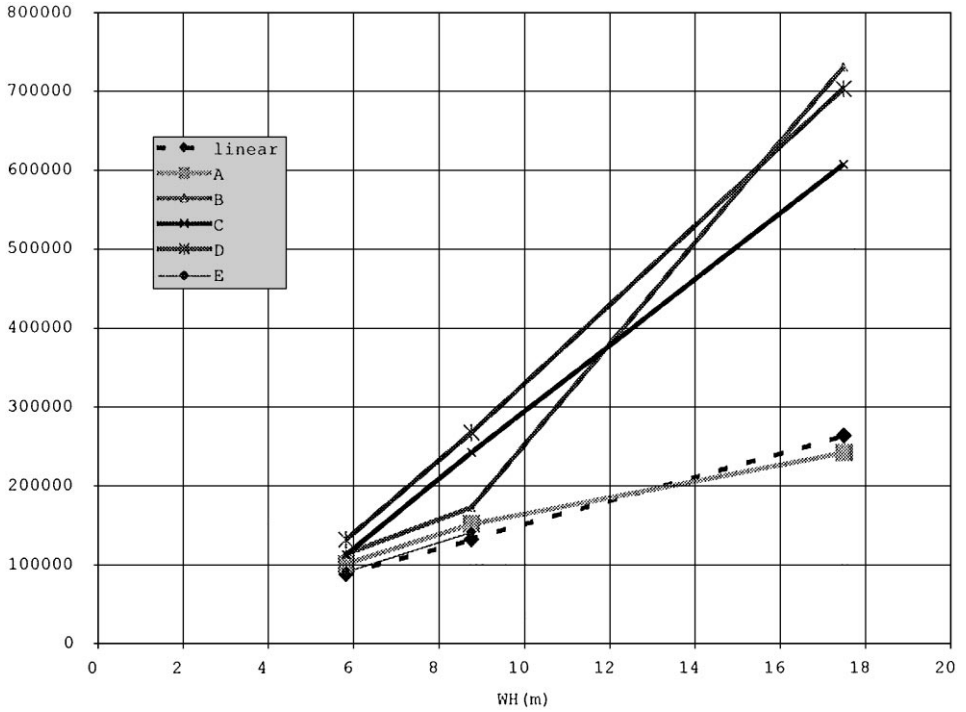


Fig. 5. Variation of midship vertical bending moment to the wave height wave length ratio = 1.

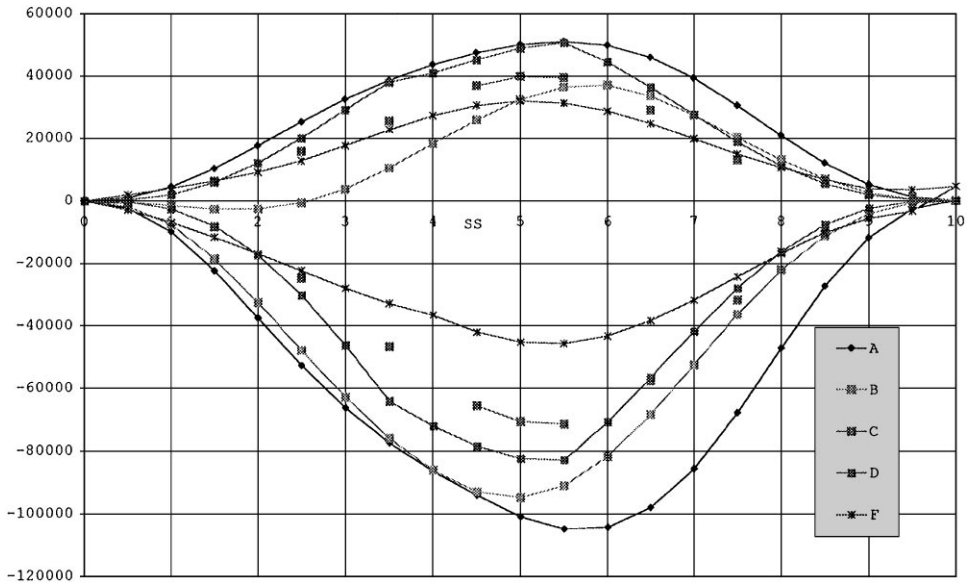


Fig. 6. Longitudinal distribution of maximum hogging and sagging moment wave length ratio = 1, wave height ratio = 1/30.

of whipping modes superposition may cause big difference in total moment peak values.

#### 4.3. Time history

Comparison was also made among the computed time histories in order to examine the program's ability to estimate temporal and phase characteristics of the responses. Firstly, the relative wave motion at the FP is examined. Fig. 7 shows estimated time histories in a wave with wave length ratio 1 and Fig. 8 shows those of wave length of 2. The time histories from six programs are shown here. The time origin in the graphs is taken at the moment when the pitching crosses zero in the bow-up direction. The wave height in these cases is 1/30 of the wavelength. It is seen that they have almost identical phase relation each other and hence to the pitching motion.

Turning to the behaviour of the wave bending moment. Figs. 9 and 10 show the time histories of VBM at the midship in the same cases as in the relative wave motion above. Most of the computed results show good agreement with each other in magnitude and temporal shape as far as fundamental period component is concerned. But for the whipping vibration component they give diversified estimation to the extent that even the vibration period is different.

When the wave height becomes higher, the difference of the programs is pronounced. Figs. 11–13 show time histories of the midship vertical bending moment calculated by three programs A, B and C for different wave height with wave length

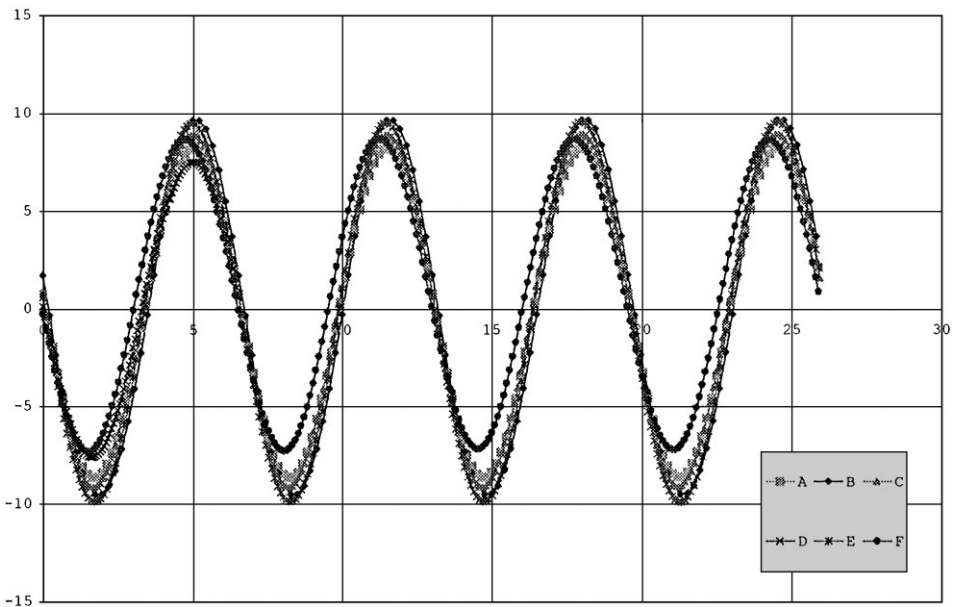


Fig. 7. Time histories of relative water elevation at FP wave length ratio = 1, wave height ratio = 1/30.

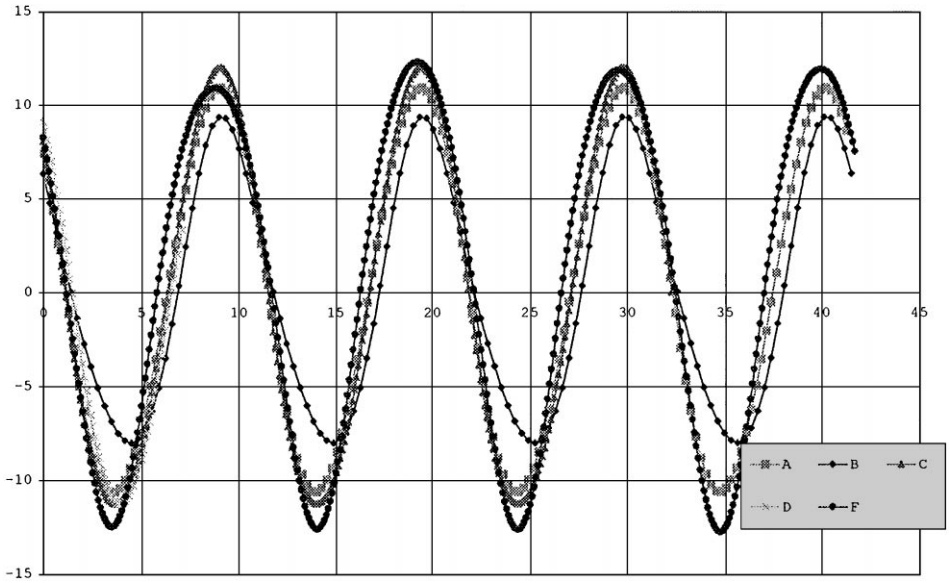


Fig. 8. Time histories of relative water elevation at FP wave length ratio = 2, wave height ratio = 1/30.

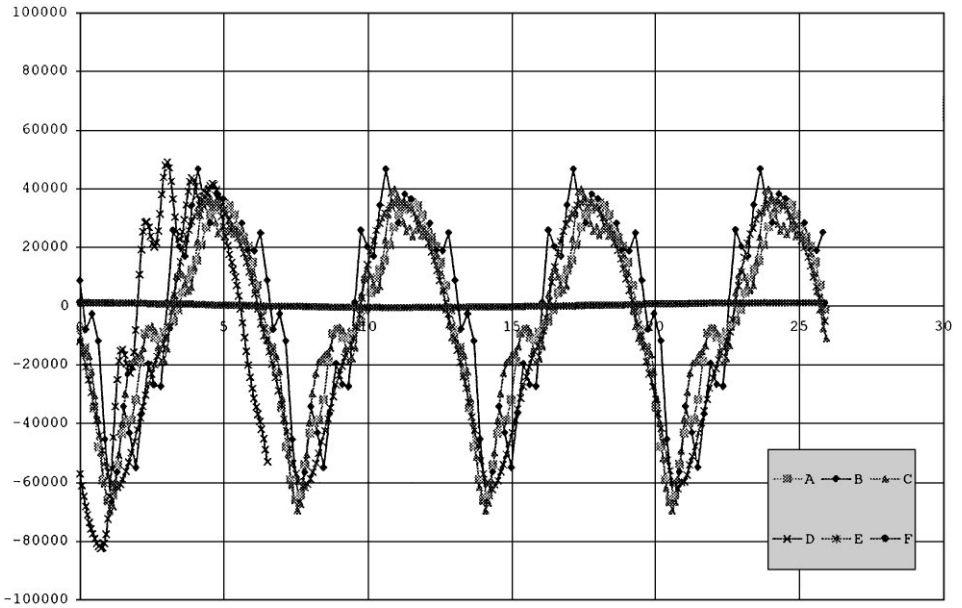


Fig. 9. Time histories of midship vertical bending moment wave length ratio = 1, wave height ratio = 1/30.

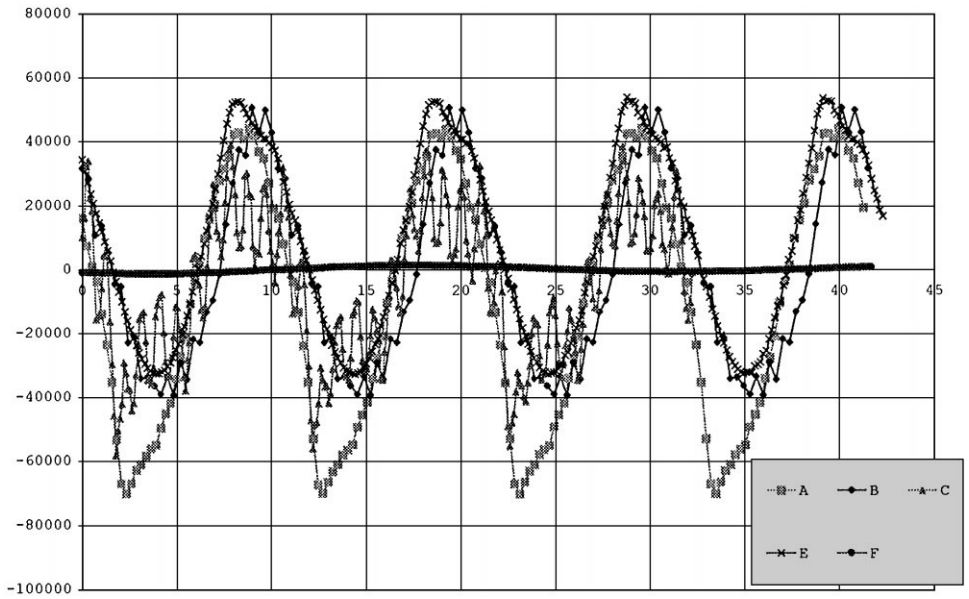


Fig. 10. Time histories of midship vertical bending moment wave length ratio = 2, wave height ratio = 1/30.

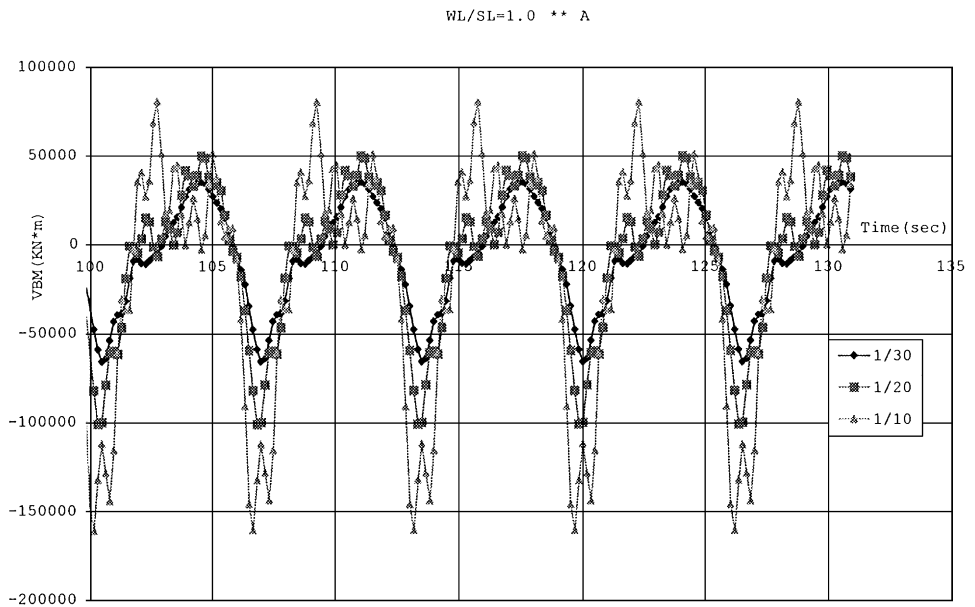


Fig. 11. Time histories of midship vertical bending moment by program A wave length ratio = 1, wave height ratio = 1/30, 1/20, 1/10.

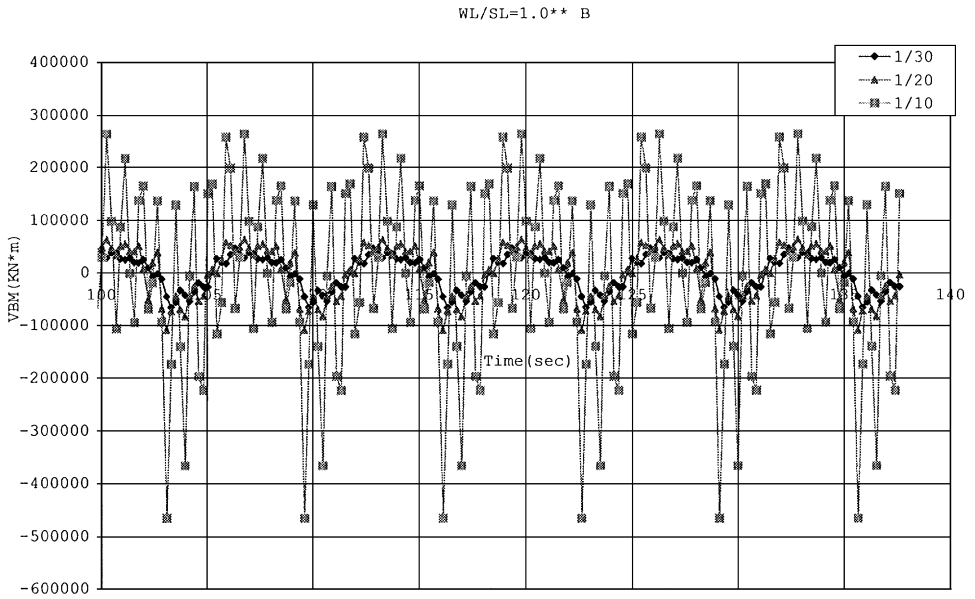


Fig. 12. Time histories of midship vertical bending moment by program B wave length ratio = 1, wave height ratio = 1/30, 1/20, 1/10.

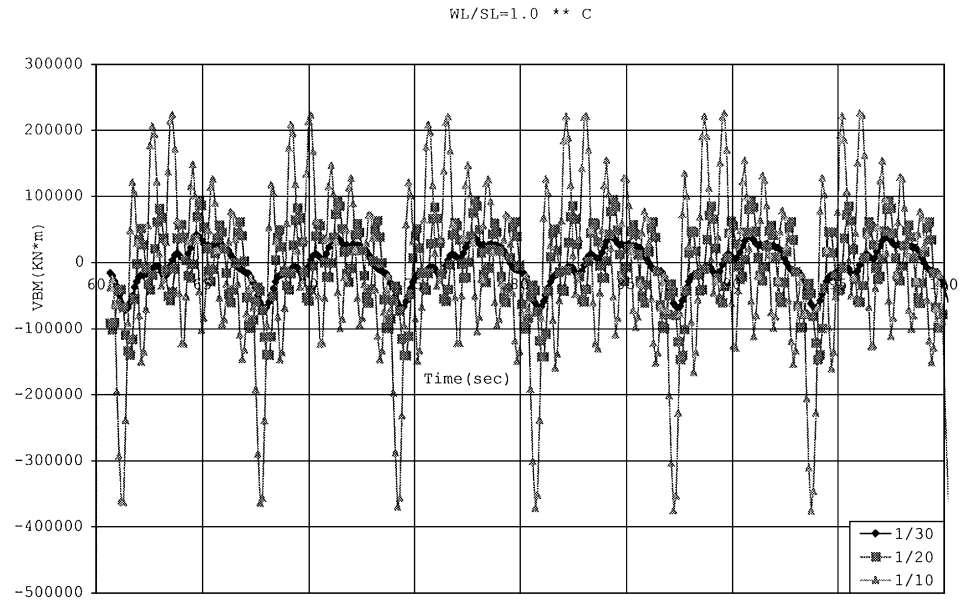


Fig. 13. Time histories of midship vertical bending moment by program C wave length ratio = 1, wave height ratio = 1/30, 1/20, 1/10.



ratio of 1. It is clear that the bending moment shows different behaviour for the higher wave height from program to program. The difference in vibratory characteristics is pronounced when the wave height becomes higher. The program A gives the most sustained vibration whereas the program B and C give stronger vibration even if these three give similar fundamental period component. Moreover the vibration given by C is much damped in spite of the peak values being in the same order.

## 5. Conclusions

Only a limited number of codes were used for the comparison because of time limitations. Despite that, the general trend clearly indicates the following points. All methods give results that are consistent with the linear estimates in the lower wave height region. However the agreement among the computed values becomes poor in the higher wave region when elastic behaviour plays a significant role.

A further step would be to make comparisons with experimental or measured data in order to decide whether the non-linear programs are reliable tools for predicting the wave-induced loads and responses of a ship in waves. More efforts should be put to this end.

## Acknowledgements

Thanks are due to A. Incecik (Newcastle University), N. Fonseca (Instituto Superior Técnico), J. Ramos (Instituto Superior Técnico), A. Nestergaard (Det Norske Veritas), J. Shen (China Ship Scientific Research Centre) and T. Fukawasa (Kanazawa Institute of Technology) for having performed the calculations reported here, within the time constraints of the study.

Special thanks are due to Nuno Fonseca for his help in collecting some material for this paper.

## References

- [1] Guedes Soares C, Dogliani M, Ostergaard C, Parmentier G, Pedersen PT. Reliability based ship structural design. *Trans. SNAME*, 1996;104:357–89.
- [2] Guedes Soares C. Effect of transfer function uncertainty on short term ship responses. *Ocean Eng* 1991;18(4):329–62.
- [3] Smith CS. Measurement of service stresses in warships. *Conference on Stresses in Service*. London: Inst. of Civil Engrs, 1966. p. 1–8.
- [4] Lin WM, Meinhold M, Salvesen N, Yue DKP. Large amplitude motions and wave loads for ship design. *Proceedings 20th Symposium on Naval Hydrodynamics*. Santa Barbara, CA, 1994.
- [5] Lin WM, Zhang S, Yue DKP. Linear and non-linear analysis of motions and loads of a ship with forward speed in large-amplitude waves. *Proceedings 11th International Workshop on Water Waves and Floating Bodies*. Hamburg, Germany, 1996.
- [6] Scorpio, SM, Beck, RF, Korsmeyer FT. Non-linear water wave computations using a multipole accelerated, desingularized method. *Proceedings 21st Symposium on Naval Hydrodynamics*. Trondheim, 1996. p. 34–43.

- [7] Beck R, Cao Y, Scorpio S, Schultz W. Non-linear ship motions computations using the desingularized method. Proceedings 20th Symposium on Naval Hydrodynamics. Santa Barbara, California, 1994.
- [8] Zhao R, Aarsnes V. Numerical and experimental studies of non-linear motions and loads of a high-speed catamaran. Proceedings of the third International Conference on Fast Sea Transportation. Lübeck-Travemünde, Germany, 1995. p. 1017–30.
- [9] Fonseca N, Guedes Soares C. Time-domain simulation of vertical ship motions. In: Murthy TKS, Wilson PA, Wadhams P, editors. Marine offshore and ice technology. Southampton: Computational Mechanics Publications, 1994. p. 224–43.
- [10] Fonseca N, Guedes Soares C. Time-domain analysis of large-amplitude vertical motions and wave loads. *J Ship Res.* 1998;42(2):100–13.
- [11] Xia J, Wang Z, Gu X, Shen J, Wu Y. Numerical simulation of the wave-induced non-linear bending moment of ships. Proceedings of the 14th Conference on Offshore Mechanics and Arctic Engineering, 1995. vol. II. pp. 147–53.
- [12] Watanabe I, Sawada H. Effects of elastic responses to the longitudinal bending moment in two-directional waves. *Naval Architecture Mar Eng.* 1986;24:91–102.
- [13] Tao Z, Incecik A. Non-linear motions and global bending moments in regular head seas. In: Murthy TKS, Wilson PA, Wadhams P, editors. Marine offshore and ice technology. Southampton: Computational Mechanics Publications, 1994.
- [14] Tao Z, Incecik A. Time-domain simulation of vertical ship motions and loads in regular head seas. Proceedings of the 17th International Conference on Offshore Mechanics and Arctic Engineering. New York: ASME, 1998. 98–591
- [15] Ramos J, Guedes Soares C. Vibratory response of ship hulls to wave impact loads. *Int Shipbuilding Prog* 1998;45(441):71–8.
- [16] Kring DC, Huang YF, Scavonous PD, Vada T, Braathen A. Non-linear ship motions and wave-induced loads by a rankine panel method. Proceedings of 21st Symposium on Naval Hydrodyn, Trondheim, 1996. p. 16–33.
- [17] Yamamoto Y, Fujino M, Fukasawa T, Ohtsubo H. Slamming and whipping of ships among rough seas. Numerical analysis of the dynamics of ship structures. Proceedings of EUROMECH Colloquium 122, Paris, 1979, p. 19–33.